

Organic light-emitting materials based on iridium(III) complexes bearing phenanthroimidazole ligands

Jayaraman Jayabharathi^{a*}, Ramalingam Sathishkumar^a and Venugopal Thanikachalam^a

We present the elegant synthesis and the photophysical and electroluminescent properties of a series of cyclometalated iridium(III) complexes [Ir(PPI)₂(pic), PPI: 1,2-diphenyl-1H-phenanthro[9,10-d]imidazole; pic: picolinic acid]. The Ir(PPI)₂(pic) complexes showed characteristic phosphorescence with an emission range of 556–579 nm and a high quantum efficiency with microsecond lifetimes. The strongly allowed phosphorescence in these complexes is the result of significant spin-orbit coupling of the Ir center. All bis(PPI) derivatives exhibit intense triplet metal-to-ligand charge transfer (MLCT) photoluminescence in the fluid solutions at room temperature. The impact of different solvents, substituents on the phenanthroimidazole ligands and complex concentrations upon their emissive behavior have been examined and demonstrate that their emission energies can be systematically modified. Weak bands located at longer wavelength have been assigned to the ¹MLCT ← S₀ and ³MLCT ← S₀ transitions of iridium complexes. Application of the ³MLCT excited state of the [Ir(PPI)₂(pic)] materials in organic light-emitting devices are described. Copyright © 2014 John Wiley & Sons, Ltd.

Keywords: charge transfer; electroluminescence; iridium complex; phosphorescence

INTRODUCTION

Cyclometalated iridium(III) complexes have attracted considerable attention in material research due to their outstanding performance in organic light-emitting diodes (OLED).^[1–4] The strong spin-orbit coupling induced by a heavy-metal ion promotes an efficient intersystem crossing (ISC) between the singlet and the triplet excited state manifold. Therefore, both singlet and triplet excitons can be harnessed, and then strong electroluminescence with an internal efficiency theoretically approaching to 100% can be achieved.^[5–8] Host materials in phosphorescent organic light-emitting diodes (PhOLEDs) have drawn intensive attention owing to their capability to prevent triplet-triplet annihilation and concentration quenching effect.^[9–11] The Ir(III) complexes reported generally contain two cyclometalated ligands and a bidentate, monoanionic ancillary ligand, or with three cyclometalated ligands. Both the luminescent efficiency and emission colors of Ir(III) complexes can be tuned by introduction of substituents with different electronic effects or variations of the conjugation system on ligands.^[12–16]

The energy gap of the synthesized complex has been tuned by incorporating the substituents in the ligand to obtain the desired emission. Thus, manipulation of the skeletal arrangement as well as the substituent groups of the cyclometalating ligand may represent a promising venue for the development of highly phosphorescent Ir(III) complexes. Although a wide range of Ir(III) materials have been reported, the number of highly phosphorescent imidazole-based cyclometalated Ir(III) complexes is still rare.^[17,18] 1,3,5-Tris(N-phenylbenzimidazole-2-yl)-benzene, a commonly used electron transporter and hole blocker, is a derivative of benzoimidazole compounds. Therefore, benzoimidazole(bi)-based cyclometalated iridium complexes may have good electron transporting ability, which is highly desirable in designing

high-efficiency OLEDs.^[16] Our interest in the development of highly efficient phosphors for application in OLEDs has prompted us to synthesize iridium complexes and investigate their photophysical and electroluminescent characteristics.

Herein, we discuss a series of iridium(III) bis(PPI) complexes with picolinic acid (pic) as ancillary ligands (Scheme 1). By varying the substituents, we have been able to fine-tune their ³MLCT excited-state properties. These complexes are strong emitters in the fluid solutions, and their electroluminescent (EL) properties have been studied in order to evaluate their suitability as OLED materials.

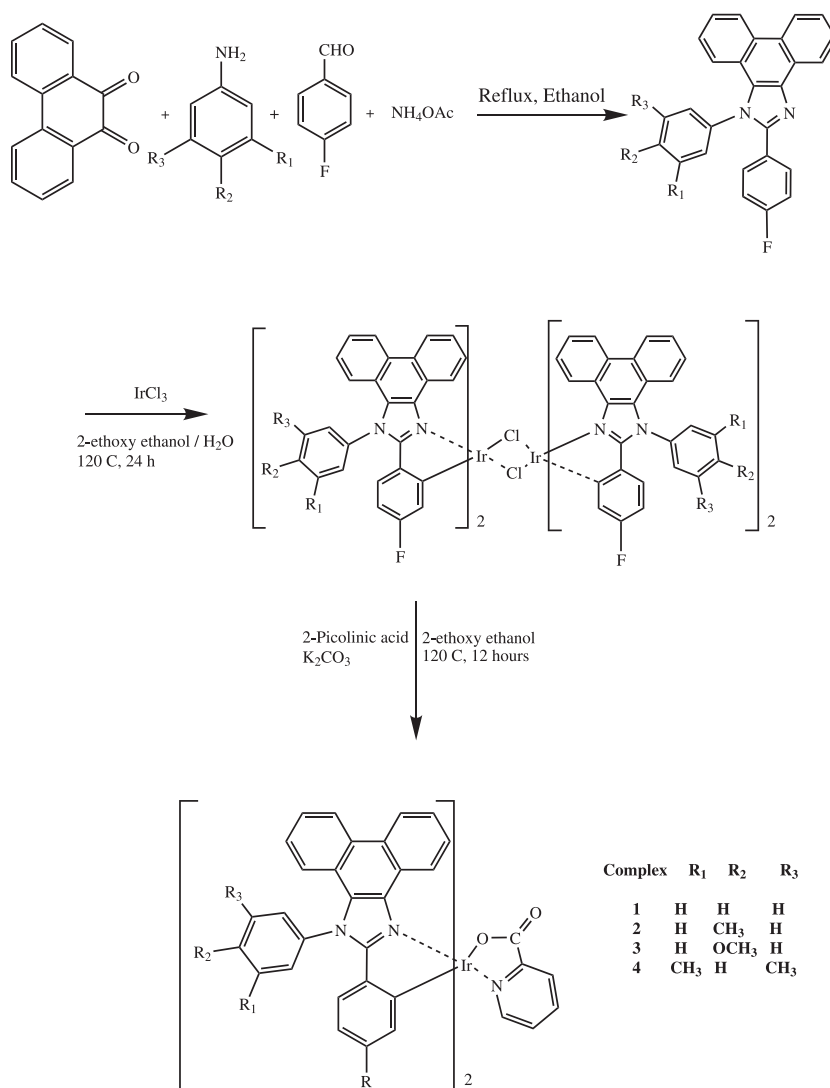
EXPERIMENTAL

Optical measurements and composition analysis

The ultraviolet-visible (UV-vis) spectra of the phosphorescent iridium complexes were measured on UV-vis spectrophotometer (Perkin Elmer Lambda 35) and corrected for background absorption due to solvent. Photoluminescence (PL) spectra were recorded on a (Perkin Elmer LS55) fluorescence spectrometer. NMR spectra were recorded on Bruker 400-MHz NMR spectrometer. The mass spectra of the samples were obtained using a Thermo Fischer LC-Mass spectrometer in fast atom bombardment mode. Cyclic voltammetry analysis was performed by using CHI 630A potentiostat electrochemical analyzer. Measurements of oxidation and reduction were undertaken using 0.1 M tetra(n-butyl) ammonium-hexafluorophosphate as the supporting electrolyte, at scan

* Correspondence to: Dr. J. Jayabharathi, Professor of Chemistry, Department of Chemistry, Annamalai University, Annamalainagar 608 002, Tamilnadu, India. E-mail: jtchalam2005@yahoo.co.in

a J. Jayabharathi, R. Sathishkumar, V. Thanikachalam
Department of Chemistry, Annamalai University, Annamalainagar 608 002, Tamilnadu, India



Scheme 1. Synthetic route of iridium complexes 1–4

rate of 0.1 V s^{-1} . The potentials were measured against an Ag/Ag⁺ (0.01 M AgNO₃) reference electrode using ferrocene/ferrocenium (CP₂Fe/CP₂Fe⁺) as the internal standard. The onset potentials were determined from the intersection of two tangents drawn at the rising current and background current of the cyclic voltammogram. All calculations were performed using density functional theory (DFT) as implemented in the with Gaussian-03 program using the Becke3-Lee-Yang-Parr (B3LYP) functional supplemented with the standard 6-31G (d, p) basis set.^[19]

Fabrication of OLEDs

The EL devices based on the iridium (III) complexes were fabricated by vacuum deposition of the materials at 5×10^{-6} Torr onto a clean glass precoated with a layer of indium tin oxide (ITO) as the substrate. The glass was cleaned by sonication successively in a detergent solution, acetone, methanol and deionized water before use. Organic layers were deposited onto the substrate at a rate of 0.1 nm s^{-1} . LiF and Alq₃ were thermally evaporated onto the surface of organic layer. The thickness of the organic materials and the cathode layers was controlled using a quartz crystal thickness monitor. A series of devices (I, II, III and IV) configuration ITO/NPB (30 nm)/iridium complex: CBP (7%) (30 nm)/BCP (10 nm)/Alq (40 nm)/Mg:Ag, was fabricated, and measurements of current, voltage and light intensity were made simultaneously using a Keithley 2400 sourcemeter. The EL spectra and luminance of the devices were carried out in ambient atmosphere without further encapsulations.

General procedure for the synthesis of iridium complexes

A mixture of phenanthrene-9, 10-dione (40 mmol), ammonium acetate (30 mmol), 4-fluorobenzaldehyde (30 mmol) and aniline (30 mmol) was refluxed in ethanol at 80 °C in the presence of indium (III) fluoride (InF₃) as Lewis acid catalyst for 30 min which yields the phenanthroimidazole (PPI) derivatives. The phenanthroimidazole-based cyclometalated iridium complexes have been synthesized via Nonoyama route^[20] (Scheme 1).

Iridium(III)bis(2-(4-fluorophenyl)-1-phenyl-1H-phenanthro [9,10-d]imidazolato-N,C^{2'}) (picolinate), [Ir(fppi)₂(pic)], (1)

Yield: 88%. ¹H NMR (400 MHz, CDCl₃): δ 9.16 (d, 1H, J = 8.0 Hz), 8.61 (dd, 2H, J = 8.4 Hz), 8.50 (d, 1H, J = 8.0 Hz), 8.45 (d, 1H, J = 8.8 Hz), 8.39 (d, 1H, J = 7.6 Hz), 8.27 (d, 1H, J = 6.4 Hz), 8.08 (d, 1H, J = 8.0 Hz), 7.87–7.94 (m, 6H), 7.78 (t, 1H, J = 7.2 Hz), 7.71 (d, 1H, J = 7.6 Hz), 7.66 (d, 1H, J = 6.8 Hz), 7.61 (t, 1H, J = 8.0 Hz), 8.45 (d, 1H, J = 8.8 Hz), 7.46–7.53 (m, 5H), 7.39 (t, 1H, J = 6.0 Hz), 8.45 (d, 1H, J = 8.8 Hz), 7.18–7.25 (m, 4H), 7.12 (d, 1H, J = 8.0 Hz), 7.06 (d, 1H, J = 8.4 Hz), 7.03 (d, 1H, J = 8.4 Hz), 6.69 (t, 1H, J = 7.2 Hz), 6.63 (d, 1H, J = 9.2 Hz), 6.32–6.44 (m, 4H). ¹³C NMR (100 MHz, CDCl₃): δ 108.29, 108.53, 108.68, 108.91, 120.26, 120.50, 121.84, 121.98, 122.13, 122.39, 122.89, 123.39, 123.56, 123.99, 124.14, 124.40, 125.29, 125.44, 125.77, 125.65, 125.72, 126.09, 126.19, 126.46, 126.68, 126.76, 126.78, 127.00, 127.40, 127.51, 128.47, 128.53, 128.74, 128.84, 129.23, 129.72, 129.94, 130.92, 131.09, 131.22, 131.46, 131.54, 131.70, 132.56,

133.33, 134.25, 137.49, 137.78, 146.24, 149.90, 150.66, 150.72, 152.75, 160.69, 160.80, 161.02, 162.12, 163.20, 163.54, 172.28. Anal. calcd. for $C_{60}H_{36}F_2IrN_5O_2$: C, 66.16; H, 3.33; N, 6.43. Found: C, 66.67; H, 3.59; N, 6.54. MS: m/z 1089.73 [M^+].

Iridium(III)bis(2-(4-fluorophenyl)-1-p-tolyl-1H-phenanthro [9,10-d]imidazolato-N,C^{2'}) (picolate), [Ir(ftpi)₂(pic)], (2)

Yield: 90%. ¹H NMR (400 MHz, CDCl₃): δ 9.16 (d, 1H, $J=8.0$ Hz), 8.60 (dd, 2H, $J=7.6$ Hz), 8.49 (d, 1H, $J=8.0$ Hz), 8.45 (d, 1H, $J=8.4$ Hz), 8.26 (d, 1H, $J=6.6$ Hz), 8.23 (d, 1H, $J=8.4$ Hz), 7.45–7.73 (m, 13H), 7.20–7.38 (m, 6H), 7.12 (d, 1H, $J=8.0$ Hz), 7.01 (d, 1H, $J=9.2$ Hz), 6.70 (t, 1H, $J=7.2$ Hz), 6.62 (d, 1H, $J=9.6$ Hz), 6.44–6.49 (m, 3H), 6.36 (t, 1H, $J=8.4$ Hz), 2.68 (s, 3H), 2.71 (s, 3H). ¹³C NMR (100 MHz, DMSO): δ 21.74, 21.80, 108.22, 108.45, 108.62, 108.85, 120.31, 120.56, 121.75, 122.10, 122.49, 122.93, 122.99, 123.33, 123.50, 123.93, 124.09, 124.35, 125.21, 125.36, 125.50, 125.70, 125.79, 126.13, 126.22, 126.41, 126.73, 126.82, 126.96, 127.01, 127.36, 127.57, 128.15, 128.44, 128.70, 128.84, 129.19, 129.55, 129.67, 131.49, 131.80, 131.87, 132.12, 132.65, 133.25, 134.20, 135.05, 135.07, 137.44, 141.28, 141.78, 146.24, 149.92, 150.58, 150.65, 152.74, 160.66, 160.86, 162.17, 163.16, 163.52, 172.28. Anal. calcd. for $C_{62}H_{40}F_2IrN_5O_2$: C, 66.65; H, 3.61; N, 6.27. Found: C, 66.78; H, 3.68; N, 6.32. MS: m/z 1117.60 [M^+].

Iridium(III)bis(2-(4-fluorophenyl)-1-(4-methoxyphenyl)-1H-phenanthro [9,10-d]imidazolato-N,C^{2'}) (picolate), [Ir(fmppi)₂(pic)], (3)

Yield: 86%. ¹H NMR (400 MHz, CDCl₃): δ 9.15 (d, 1H, $J=7.6$ Hz), 8.64 (d, 1H, $J=8.0$ Hz), 8.59 (d, 1H, $J=8.0$ Hz), 8.45 (d, 1H, $J=7.6$ Hz), 8.26 (d, 2H, $J=8.4$ Hz), 8.06 (d, 1H, $J=8.0$ Hz), 7.75 (d, 1H, $J=8.0$ Hz), 7.44–7.59 (m, 8H), 7.17–7.40 (m, 11H), 6.99 (d, 1H, $J=9.6$ Hz), 6.70 (t, 1H, $J=7.6$ Hz), 6.62 (d, 1H, $J=9.6$ Hz), 6.48–6.53 (m, 3H), 6.39 (t, 1H, $J=8.4$ Hz), 4.06 (s,

3H), 4.08 (s, 3H). ¹³C NMR (100 MHz, CDCl₃): δ 55.85, 55.94, 107.73, 107.86, 108.28, 108.50, 109.82, 115.79, 115.90, 116.17, 116.28, 116.59, 122.10, 122.94, 122.96, 123.54, 123.94, 124.11, 124.34, 125.20, 125.38, 125.50, 125.69, 126.70, 126.83, 126.93, 127.02, 127.35, 127.68, 128.23, 128.43, 128.72, 129.53, 129.69, 129.83, 130.06, 130.14, 130.24, 130.97, 137.44, 146.24, 150.02, 150.73, 152.87, 159.19, 161.07, 161.21, 161.44. Anal. calcd. for $C_{62}H_{40}F_2IrN_5O_4$: C, 64.80; H, 3.51; N, 6.09. Found: C, 64.77; H, 3.60; N, 6.15. MS: m/z 1149.53 [M^+].

2-(4-fluorophenyl)-1-(3,5-dimethylphenyl)-1H-phenanthro [9,10-d]imidazolato-N,C^{2'}) (picolate), [Ir(fdmpipi)₂(pic)], (4)

Yield: 91%. ¹H NMR (400 MHz, DMSO): δ 9.17 (d, 1H, $J=8.3$ Hz), 8.61 (dd, 2H, $J=8.4$ Hz), 8.49 (d, 1H, $J=8.3$ Hz), 8.44 (d, 1H, $J=9.6$ Hz), 8.25 (d, 1H, $J=7.2$ Hz), 8.21 (d, 1H, $J=8.1$ Hz), 7.42–7.73 (m, 13H), 7.36 (t, 1H, $J=7.2$ Hz), 7.18–7.27 (m, 5H), 7.12 (d, 1H, $J=8.4$ Hz), 7.00 (d, 1H, $J=8.0$ Hz), 6.70 (t, 1H, $J=7.2$ Hz), 6.62 (d, 1H, $J=8.0$ Hz), 6.43–6.51 (m, 3H), 6.36 (t, 1H, $J=8.1$ Hz), 2.68 (s, 6H), 2.71 (s, 6H). ¹³C NMR (100 MHz, DMSO): δ 21.71, 21.76, 29.72, 29.87, 108.21, 108.44, 108.61, 108.85, 120.31, 120.56, 121.93, 122.01, 122.49, 122.92, 123.01, 123.33, 123.50, 123.92, 124.08, 124.34, 125.20, 125.35, 125.49, 125.69, 126.40, 126.73, 126.80, 126.90, 126.99, 127.36, 127.57, 128.14, 128.43, 128.70, 128.83, 129.18, 129.67, 131.47, 131.82, 131.86, 132.10, 133.25, 134.19, 135.05, 135.07, 137.42, 160.65, 160.87, 162.18, 163.19, 172.25. Anal. calcd. for $C_{64}H_{44}F_2IrN_5O_2$: C, 67.12; H, 3.87; N, 6.11. Found: C, 67.14; H, 3.84; N, 6.15. MS: m/z 1145.47 [M^+].

RESULTS AND DISCUSSION

Absorption and emission spectra

The absorption and emission spectra of complexes **1–4** in dichloromethane at room temperature are shown in Fig. 1. The absorption bands show three kinds of bands. The intense band observed around 302 nm in the ultraviolet part of the spectrum can be assigned to the spin-allowed ligand-centered ($\pi-\pi^*$) transitions^[21] which correlate with the transition observed for free PPI and somewhat weaker bands also observed in the lower part of energy. The absorption in the range of 385–401 nm corresponds to spin-allowed $S^0 \rightarrow {}^1MLCT$ transition. The broad band appeared at in the range of 422–436 nm can be assigned to $S^0 \rightarrow {}^3MLCT$ transition and gains intensity by mixing with the higher lying 1MLCT transition through the spin-orbit coupling of iridium(III). This mixing is strong enough in this complex that the formally spin forbidden 3MLCT has an extinction coefficient that is almost equal to the spin-allowed 1MLCT transition (Fig. 2).^[17,22] Both singlet MLCT (1MLCT) and triplet MLCT (3MLCT) bands are typically observed for these

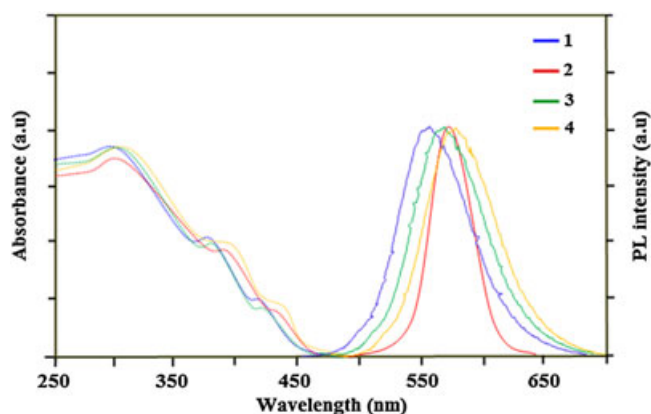


Figure 1. Absorption and emission spectra of **1–4** in CH_2Cl_2

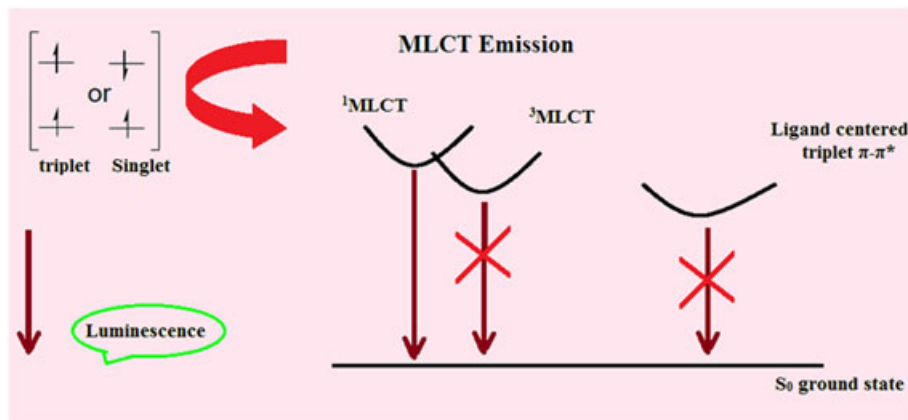


Figure 2. Spin-orbit coupling of heavy-metal facilitated triplet emission

complexes in all solvents. In order for these iridium(III) complexes to be useful as phosphor EL devices, strong spin-orbit coupling must be present to efficiently mix the singlet and triplet excited states. Clear evidences for mixing of the singlet and triplet excited states are seen in the absorption of these complexes.

Mixing of excited states (LC and MLCT)

Phosphorescence of mononuclear metal complexes originates from the ligand-centered excited state (LC), metal-centered excited state and MLCT excited state. For the cyclometalated iridium complexes, the wave function of the excited triplet state Φ_T , responsible for the phosphorescence, is expressed as,

$$\Phi_T = a\Phi_T(\pi - \pi^*) + b\Phi_T(\text{MLCT}) \quad (1)$$

where "a" and "b" are the normalized coefficient, $\Phi_T(\pi - \pi^*)$ and $\Phi_T(\text{MLCT})$ are the wave function of ${}^3(\pi - \pi^*)$ and ${}^3(\text{MLCT})$ excited states, respectively. For these iridium complexes, the wave function of the triplet state (Φ_T) responsible for the phosphorescence and Eqn (1) implies that the excited triplet state of these iridium complexes is a mixture of $\Phi_T(\pi - \pi^*)$ and $\Phi_T(\text{MLCT})$.^[23] The triplet state is attributed to dominantly ${}^3\pi - \pi^*$ excited state when $a > b$ and dominantly ${}^3\text{MLCT}$ excited state when $b > a$.

The photoluminescence spectra of these complexes obtained at 298 K show a significant broad shape. According to our previous studies,^[24–26] phosphorescence spectra from the ligand-centered ${}^3\pi - \pi^*$ state display vibronic progressions, while those from the ${}^3\text{MLCT}$ state are broad in shape. Complexes **1**, **3** and **4** have excited state with large contribution of ${}^3\text{MLCT}$ whereas complex **2** have excited state with large contribution of ${}^3\pi - \pi^*$.

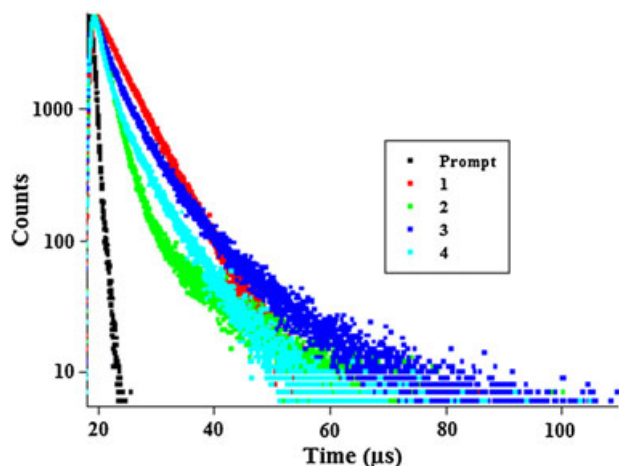


Figure 3. Lifetime spectra of **1–4** in CH_2Cl_2

Electronic transition theory

The time correlated single photon counting (TCSPC) results fit to single exponentials decay (Fig. 3); DAS6 software was used for the fit and the χ^2 values are less than 1.2. The lifetime measurements of all iridium complexes were made, and the signal was measured at the emission wavelength of individual compound. The absolute PL quantum yields were measured by comparing emission intensities (integrated areas) of a standard sample (Coumarin 46) and the unknown sample^[26,27] using the formula

$\Phi_{\text{unk}} = \Phi_{\text{std}} \left(\frac{I_{\text{unk}}}{I_{\text{std}}} \right) \left(\frac{A_{\text{std}}}{A_{\text{unk}}} \right) \left(\frac{\eta_{\text{unk}}}{\eta_{\text{std}}} \right)^2$ where, Φ_{unk} is the quantum yield of the sample, Φ_{std} is the quantum yield of the standard, I_{unk} and I_{std} are the integrated emission intensities of the sample and the standard, respectively. A_{unk} and A_{std} are the absorbances of the sample and the standard at the excitation wavelength, respectively. η_{unk} and η_{std} are the indexes of refraction of the sample and standard solutions.^[23] The radiative and non-radiative decay of the excited state of iridium complexes has been obtained using the quantum yields and lifetimes and is listed in Table 1. Moreover, radiative lifetime of these complexes falls in the range of 0.59–0.92 μs . The formula employed to calculate the radiative (k_r) and non-radiative (k_{nr}) rate constants is $\Phi_{\text{p}} = \Phi_{\text{ISC}} \{k_r / (k_r + k_{nr})\}$; $k_r = \Phi_{\text{p}} / \tau$; $k_{nr} = (1/\tau) - (\Phi_{\text{p}}/\tau)$; $\tau = (k_r + k_{nr})^{-1}$, where, here, Φ_{ISC} is the intersystem-crossing yield. For the iridium complexes, Φ_{ISC} is safely assumed to be 1.0 because of the strong spin-orbit interaction caused by heavy atom effects of iridium.^[28] k_r and k_{nr} are the radiative and non-radiative deactivation; τ_f is the lifetime of the T_1 excited state. Perusal of the radiative and non-radiative rate constants shows that in most of the cases the radiative emission is predominant over non-radiative transitions.

Effect of substituent on tuning wavelength

Substituent effect of the d orbital (t_{2g}) stabilizes iridium(III) through the carbon atom-iridium bonding, and this identifies with the inductive effect of the substituents. Therefore, the highest occupied molecular orbital (HOMO) stability and the emission energy gap are controlled by the nature and number of substituent and its inductive influence on the aromatic ring. The photophysical study of these complexes demonstrates that the electron withdrawing substituents increase the absorption and emission energies of complexes by stabilizing the HOMO level. Besides increasing the emission energy, the lower HOMO energies decrease the energy separation between the ${}^1\text{MLCT}$ and ${}^3\text{LC}$ states, which in turn modified the excited-state properties of the iridium complexes. The complexes **1–4** undergo a reversible one-electron oxidation wave of 0.91 V vs Fc^+/Fc ^[29] in CH_2Cl_2 , which can be attributed to metal-centered $\text{Ir}^{\text{III}}/\text{Ir}^{\text{IV}}$ oxidation process. As revealed previously by electrochemical studies and

Table 1. Absorption (λ_{abs} , nm), emission (λ_{emi} , nm), fluorescence quantum yield (Φ), lifetime (τ , μs), radiative rate constant (k_r , 10^6 s^{-1}), nonradiative rate constant (k_{nr} , 10^6 s^{-1}) and electrochemical behavior of **1–4**

Complex	λ_{abs}	λ_{emi}	Φ	τ	k_r	k_{nr}	E_{onset}	$E_{\text{oxi}}^{1/2}$ (V)	HOMO (eV)	LUMO (eV)	E_g
1	298, 385, 422	556	0.56	0.59	0.95	0.74	452	0.81	5.61	2.87	2.74
2	303, 397, 434	572	0.54	0.68	0.79	0.68	441	0.83	5.63	2.82	2.81
3	299, 389, 426	567	0.58	0.78	0.74	0.54	443	0.79	5.59	2.79	2.80
4	308, 401, 436	579	0.59	0.92	0.64	0.45	457	0.75	5.55	2.84	2.71

theoretical calculations, the oxidation occurred mainly at the Ir metal cationic site, together with a minor contribution from the cyclometalated phenyl fragment.^[30] Variations of cyclometalated ligands, including replacement of pyridine by other heteroaromatic rings and incorporation of substituents on the rings, were shown to affect the oxidation potential of the iridium ion in congeners of (ppy)₂Ir(acac).^[31] Accordingly, replacing the benzoimidazole fragment with a phenanthro[9,10-d]imidazolyl moiety would significantly affect the electrochemical property of this complex. However, the oxidation potential of these complexes **1–4** appears to be only slightly higher (10 mV) than that of Ir(bi)₂(acac), showing that the metal localized HOMOs are at very similar energies. According to the equation $E_g = E_{\text{LUMO}} - E_{\text{HOMO}} = 1239/\lambda_{\text{onset}}$ (eV) and $E_{\text{HOMO}} = -E_{\text{OX}} - 4.80$ eV,^[32] the HOMO and LUMO levels of complexes **1–4** were calculated to be -5.61 , -5.63 , -5.59 , -5.55 and -2.87 , -2.82 , -2.79 , -2.84 eV respectively. This is consistent with the reported electrochemical studies and theoretical calculations that the one-electron oxidation of such d₆ complexes would mainly occur at the metal site, together with a minor contribution from the surrounding chelates.^[30] The 3D orbitals of HOMO and lowest unoccupied molecular orbital (LUMO) of complex **1** are shown in Fig. 4. The calculated energies of the HOMO and LUMO are given in Table 1. The iridium complexes HOMO and LUMO energies were calculated based on the HOMO energies and the lowest-energy absorption edges of the absorption spectra.^[33] From the energy gap values, it was concluded that all the reported dopant (**1–4**) are green emitters.

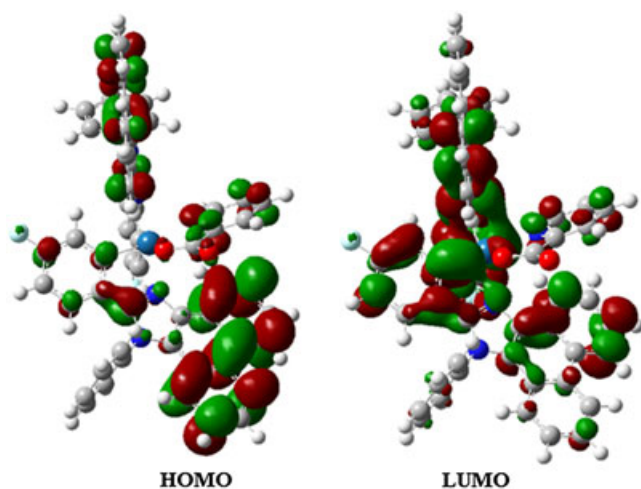


Figure 4. HOMO–LUMO orbital pictures of **1**

Description of the structure of **1**

The selected bond lengths and bond angles of **1** are presented in Table 2, and the optimization has been obtained using density functional theory (DFT/B₃LYP/6-31 (d,p)). This complex exhibits an octahedral geometry around metal iridium and prefers *cis*-C,C and *trans*-N,N chelate disposition instead of *trans*-C,C and *trans*-N,N chelate. Electron-rich phenyl rings normally exhibit very strong influence and *trans* effect. Therefore, the *trans*-C,C arrangement is expected to be thermodynamically higher in energy and kinetically more labile. This well-known phenomenon has been referred to as “transphobia”.^[34] The Ir–C bonds of the complex **1**, i.e. Ir–C_{av} = 2.038 Å is shorter than Ir–N bonds, i.e. Ir–N_{av} = 2.060 Å. The Ir–O bond length [2.138 Å] is longer than the mean Ir–O bond length (2.088 Å) reported^[35], and these observations reflect the *trans* influence of the phenyl groups. All other bond lengths and bond angles are analogous to the similar type of complexes (Fig. 5).

Thermal studies

The thermal properties of the iridium complexes **1–4** have been investigated by differential scanning calorimetry (DSC) and thermal gravimetric analyses (TGA) under nitrogen atmosphere and displayed in Fig. 6. TGA and DSC measurements have shown that iridium complexes **1–4** are a highly thermally stable material. Thermal decomposition temperature (T_{d5}), defined as the temperature at which the material showed a 5% weight loss, has been measured to be 378, 383, 369 and 386 °C for compounds **1**, **2**, **3** and **4**, respectively. Its glass transition temperature (T_g) is in the range of 115 to 129 °C.

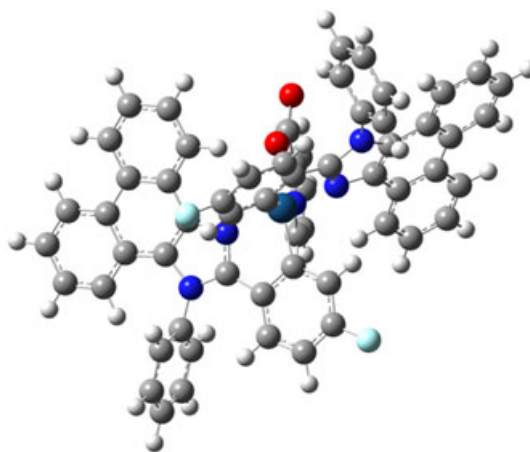


Figure 5. Optimized structure of **1**

Table 2. Selected bond lengths (Å) and bond angles (°) of **1** by DFT/B₃LYP/6-31 (d,p)

Bond lengths (Å)	DFT/B ₃ LYP/6-31 (d,p) (Å)	Bond angles (°)	DFT/B ₃ LYP/6-31 (d,p) (°)
Ir(1)–C(2)	2.0075	C(2)–Ir(1)–C(9)	92.58
Ir(1)–C(9)	2.0208	C(3)–C(7)–F(85)	117.71
C(31)–N(29)	1.4146	C(10)–C(13)–F(86)	117.84
C(13)–F(86)	1.4084	N(34)–C(32)–N(36)	109.98
C(7)–F(85)	1.4071	O(39)–C(37)–O(38)	126.54
C(37)–O(39)	1.3226	C(37)–C(19)–N(18)	117.25

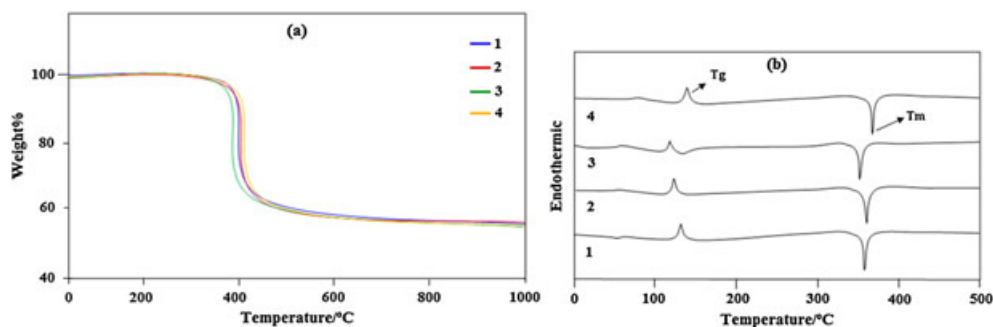


Figure 6. (a) TG-DTA curves of 1–4; (b) DSC curves of 1–4

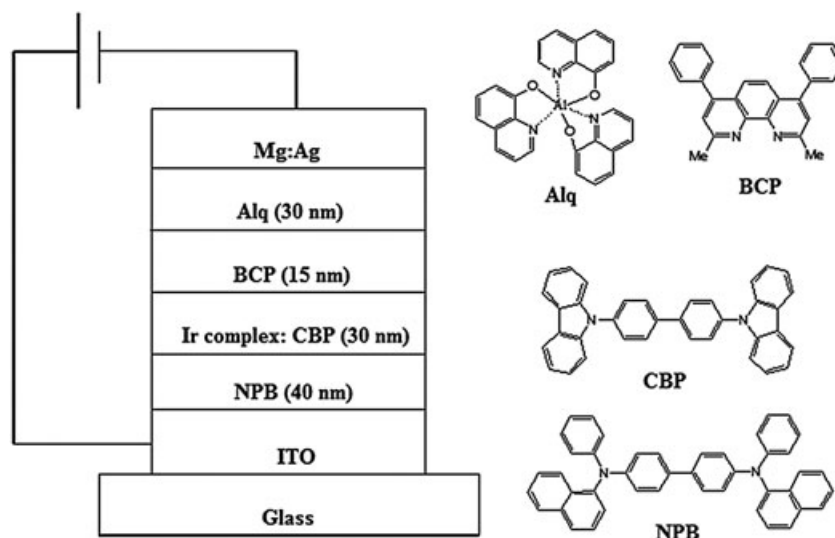


Figure 7. General structure of device

Table 3. Performances of electroluminescence devices I–IV

Device	V_d (V)	L_{\max} (cd/m ²)	η_{ext} (%)	η_c cd/A	η_p (lm/W)	EL _{max} (nm)
I	3.2	11 430, 11 V	8.3, 6 V	32.6, 6 V	25.0, 5 V	559
II	5.0	15 260, 12 V	6.0, 10 V	21.6, 9.5 V	8.7, 10 V	575
III	3.5	19 803, 11 V	13.0, 8 V	41.3, 8 V	25.3, 6 V	570
IV	3.2	24 356, 11 V	14.2, 8 V	40.8, 8 V	20.6, 7 V	580

V_d : driving voltage; L_{\max} : luminous efficiency; η_c : current efficiency; EL_{max}: electroluminescence maxima; η_p : power efficiency; η_{ext} : external quantum yield

The melting point (T_m) of compounds 1, 2, 3 and 4 measured by DSC examinations is 380, 381, 370 and 385 °C, respectively. The high T_m and T_{d5} values indicate that the compounds 1–4 are thermally stable and are able to undergo the vacuum thermal sublimation process. Therefore, these derivatives could be used in EL devices since the high T_m and T_g values improve the lifetime of the devices.

Electroluminescent properties

To demonstrate the electroluminescent properties of iridium complexes, typical OLED devices using the prepared iridium complexes as dopants have been fabricated (Fig. 7). The devices had a multi-layer configuration ITO/NPB (30 nm)/iridium complex: CBP (7%) (30 nm)/BCP (10 nm)/Alq (40 nm)/Mg:Ag, in which ITO was used

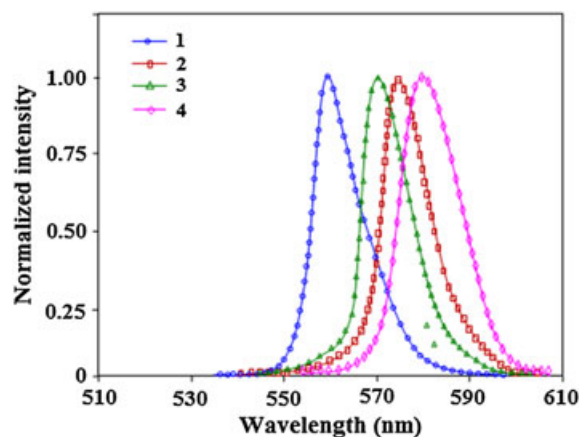


Figure 8. Electroluminescence spectra of 1–4 in CH₂Cl₂

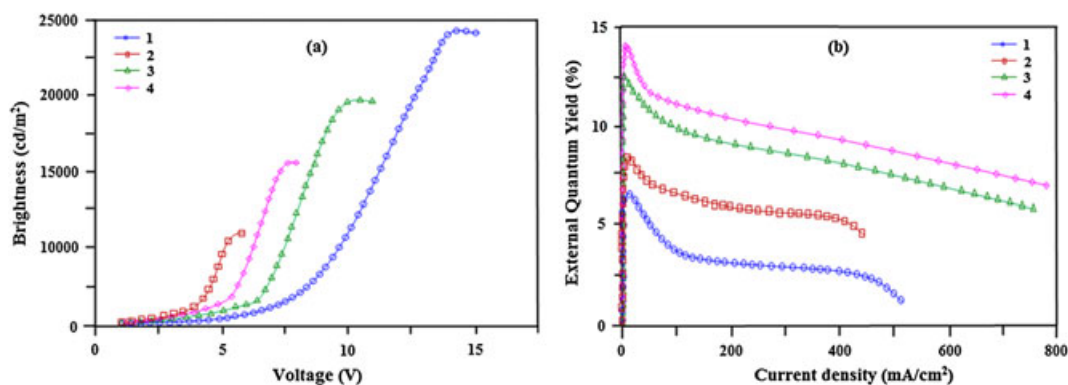


Figure 9. (a) Plot of brightness vs voltage; (b) plot of external quantum yield vs current density

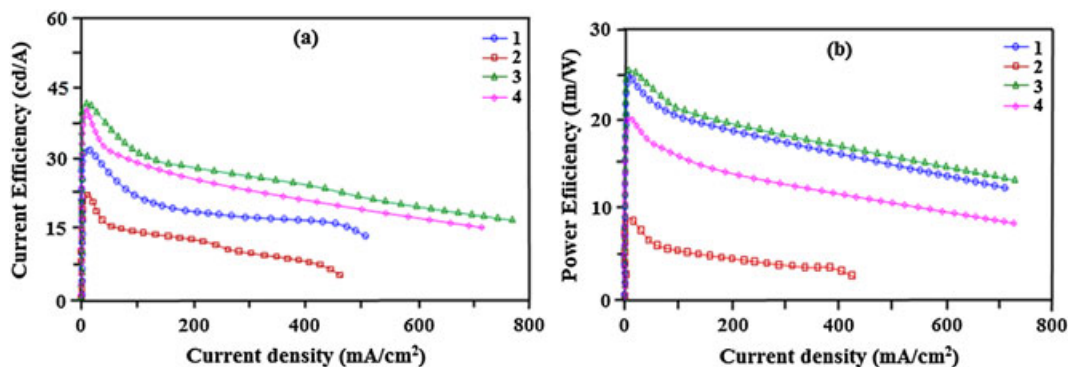


Figure 10. (a) Plot of current efficiency vs current density; (b) plot of power efficiency vs current density

as the anode, NPB (4,40-bis[N-(1-naphthyl)-N-phenylamino]biphenyl) was used as the hole-transporting material, CBP (4,40-N,N0-dicarbazole biphenyl) as the host, the iridium complexes as the dopant, BCP (2,9-dimethyl-4,7-diphenyl-1,10-phenanthroline) as the hole blocker, Alq (tris(8-hydroxyquinolino)aluminium) as the electron transporter and Mg:Ag as the cathode. Key characteristics of these devices are listed in Table 3. The devices 1–4 emitted strong green light with an emission maximum at 559, 575, 570 and 580 nm, respectively (Fig. 8). Figures 9a and 9b show the brightness–voltage and the external quantum yield–current density characteristics of the devices, respectively. All devices show quite appreciable efficiencies and brightness. Devices III and IV show the better performance in terms of brightness and power efficiency, with brightness of 19 803 cd/m² at 11 V and 24 356 cd/m² at 11 V, respectively. Device IV with of Ir(fdmppi)₂ (pic) as dopant shows an extremely high power (Fig. 10a) and current (Fig. 10b) efficiencies of 25.3 lm/w and 7.0 V, respectively (Table 3).

CONCLUSIONS

A series of highly photoluminescent and tunable bis(1,2-diphenyl-1H-phenanthro[9,10-d]imidazole) iridium(III) complexes have been synthesized. These complexes exhibit different quantum efficiencies in solution depending upon the nature of substituents. The wavelength can be tuned by adjusting the electronic properties of the substituents in the ligand. Some of the complexes discussed here showed ³MLCT predominant mixing states for their lowest excited triplet states. But the degree of mixing between ³MLCT and

³ π – π^* states of the excited states varied. While the performance of the devices described herein are limited, we have illustrated that these iridium(III) complexes warrant further investigations as OLED materials due to their tunable emission properties and their ability to mediate efficient energy transfer.

Acknowledgements

One of the authors Prof. J. Jayabharathi is thankful to DST [No. SR/S1/IC-73/2010], DRDO (NRB-213/MAT/10-11) and CSIR (NO 3732/NS-EMRII) for providing funds to this research study.

REFERENCES

- [1] I. Avilov, P. Minoofar, J. Cornil, L. D. Cola, Influence of Substituents on the Energy and Nature of the Lowest Excited States of Heteroleptic Phosphorescent Ir(III) Complexes: A Joint Theoretical and Experimental Study, *J. Am. Chem. Soc.* **2007**, *129*, 8247–8258.
- [2] J. Y. Hung, C. H. Lin, Y. Chi, M. W. Chung, Y. J. Chen, G. H. Lee, P. T. Chou, C. C. Chen, C. C. Wu, Phosphorescent Ir(III) complexes bearing double benzyldiphenylphosphine cyclometalates; strategic synthesis, fundamental and integration for white OLED fabrication, *J. Mater. Chem.* **2010**, *20*, 7682–7693.
- [3] K. Hanson, A. Tamayo, V. V. Diev, M. T. Whited, P. I. Djurovich, M. E. Thompson, Efficient dipyrin-centered phosphorescence at room temperature from bis-cyclometalated iridium(III) dipyrinato complexes, *Inorg. Chem.* **2010**, *49*, 6077–6084.
- [4] C. F. Chang, Y. M. Cheng, Y. Chi, Y. C. Chiu, C. C. Lin, G. H. Lee, P. T. Chou, C. C. Chen, C. H. Chang, C. C. Wu, Highly Efficient Blue-Emitting Iridium(III) Carbene Complexes and Phosphorescent OLEDs, *Angew. Chem. Int. Ed.* **2008**, *47*, 4542–4545.
- [5] X. Gong, J. C. Ostrowski, G. C. Bazan, D. Moses, A. J. Heeger, M. S. Liu, A. K. Y. Jen, *Adv. Mater.* **2003**, *15*, 45.

- [6] X. W. Chen, J. L. Liao, Y. M. Liang, M. O. Ahmed, H. E. Tseng, S. A. Chen, High-Efficiency Red-Light Emission from Polyfluorenes Grafted with Cyclometalated Iridium Complexes and Charge Transport Moiety, *J. Am. Chem. Soc.* **2003**, *125*, 636–637.
- [7] Y. J. Su, H. L. Huang, C. L. Li, C. H. Chien, Y. T. Tao, P. T. Chou, S. Datta, R. S. Liu, Highly Efficient Red Electrophosphorescent Devices Based on Iridium Isoquinoline Complexes: Remarkable External Quantum Efficiency Over a Wide Range of Current, *Adv. Mater.* **2003**, *15*, 884–888.
- [8] F. C. Hsu, Y. L. Tung, Y. Chi, C. C. Hsu, Y. M. Cheng, M. L. Ho, P. T. Chou, S. M. Peng, A. J. Carty, En route to the formation of high-efficiency, osmium(II)-based phosphorescent materials, *Inorg. Chem.* **2006**, *45*, 10188–10196.
- [9] M. A. Baldo, S. Lamansky, P. E. Burrows, M. E. Thompson, S. R. Forrest, Veryhigh-efficiency green organic light-emitting devices based on electrophosphorescence, *Appl. Phys. Lett.* **1999**, *75*, 4–6.
- [10] S. J. Yeh, M. F. Wu, C. T. Chen, Y. H. Song, Y. Chi, M. H. Ho, S. F. Hsu, C. H. Chen, New dopant and host materials for blue-light-emitting phosphorescent organic electroluminescent devices, *Adv. Mater.* **2005**, *17*, 285–289.
- [11] J. An, J. Chang, J. Han, C. Im, Y. J. Yu, D. H. Choi, J. L. Jin, T. Majima, Tripletlevel-dependent photoluminescence and photoconduction properties of pi-conjugated polymer thin films doped by iridium complexes, *J. Photochem. Photobiol. A: Chem.* **2008**, *200*, 371–376.
- [12] C. H. Yang, C. C. Tai, I. W. Sun, Synthesis of a high-efficiency red phosphorescent emitter for organic light-emitting diodes, *J. Mater. Chem.* **2004**, *14*, 947–950.
- [13] J. P. Duan, P. P. Sun, C. H. Cheng, New Iridium Complexes as Highly Efficient Orange-Red Emitters in Organic Light-Emitting Diodes, *Adv. Mater.* **2003**, *15*, 224–228.
- [14] I. R. Laskar, T. M. Chen, *Chem. Mater.* **2004**, *16*, 111.
- [15] X. W. Zhang, C. L. Yang, L. Chen, K. Zhang, J. G. Qin, *Chem. Lett.* **2006**, *35*, 72.
- [16] W. S. Huang, J. T. Lin, C. H. Chien, Y. T. Tao, S. S. Sun, Y. S. Wen, Highly Phosphorescent Bis-cyclometalated Iridium Complexes Containing Benzoimidazole-based Ligands, *Chem. Mater.* **2004**, *16*, 2480–2488.
- [17] L. Q. Chen, C. L. Yang, J. G. Qin, J. Gao, D. G. Ma, Tuning of emission: Synthesis, structure and photophysical properties of imidazole, oxazole and thiazole-based iridium (III) complexes, *Inorg. Chim. Acta* **2006**, *359*, 4207.
- [18] (a) X. W. Zhang, J. Gao, C. L. Yang, L. N. Zhu, Z. A. Li, K. Zhang, J. G. Qin, H. You, D. G. Ma, Highly efficient iridium(III) complexes with diphenylquinoline ligands for organic light-emitting diodes: Synthesis and effect of fluorinated substitutes on electrochemistry, photophysics and electrol, *J. Organomet. Chem.* **2006**, *691*, 4312–4319. (b) B. Etienne, F. Simona, D. A. Filippo, Z. Xianxi, S. Rosario, G. Michael, N. Md. Khaja, Cyclometalated Iridium(III) Complexes Based on Phenyl-Imidazole Ligand, *Inorg. Chem.* **2011**, *50*, 451–462. (c) T. Bihai, M. Qunbo, L. Zhiwen, D. Yongping, Z. Qianfeng, Investigation on the Electrochemiluminescence Properties of a Series of Cyclometalated Iridium(III) Complexes Based on 2-Phenylquinoline Derivatives, *Acta Chimica Sinica*, **2012**, *70*(23), 2451–2456. (d) G. G. Shan, H. B. Li, H. Z. Sun, H. T. Cao, D. X. Zhu, Z. M. Su, Enhancing the luminescence properties and stability of cationic iridium(III) complexes based on phenylbenzoimidazole ligand: a combined experimental and theoretical study, *Dalton Trans.* **2013**, *42*, 11056–11065.
- [19] M. J. Frisch, G. W. Trucks, H. B. Schlegel, G. E. Scuseria, M. A. Robb, J. R. Cheeseman, J. A. Montgomery, Jr., T. Vreven, K. N. Kudin, J. C. Burant, J. M. Millam, S. S. Iyengar, J. Tomasi, V. Barone, B. Mennucci, M. Cossi, G. Scalmani, N. Rega, G. A. Petersson, H. Nakatsuji, M. Hada, M. Ehara, K. Toyota, R. Fukuda, J. Hasegawa, M. Ishida, T. Nakajima, Y. Honda, O. Kitao, H. Nakai, M. Klene, X. Li, J. E. Knox, H. P. Hratchian, J. B. Cross, C. Adamo, J. Jaramillo, R. Gomperts, R. E. Stratmann, O. Yazyev, A. J. Austin, R. Cammi, C. Pomelli, J. W. Ochterski, P. Y. Ayala, K. Morokuma, G. A. Voth, P. Salvador, J. J. Dannenberg, V. G. Zakrzewski, S. Dapprich, A. D. Daniels, M. C. Strain, O. Farkas, D. K. Malick, A. D. Rabuck, K. Raghavachari, J. B. Foresman, J. V. Ortiz, Q. Cui, A. G. Baboul, S. Clifford, J. Cioslowski, B. B. Stefanov, G. Liu, A. Liashenko, P. Piskorz, I. Komaromi, R. L. Martin, D. J. Fox, T. Keith, M. A. Al-Laham, C. Y. Peng, A. Nanayakkara, M. Challacombe, P. M. W. Gill, B. Johnson, W. Chen, M. W. Wong, C. Gonzalez, J. A. Pople, Gaussian, Inc., Pittsburgh PA, **2003**.
- [20] M. Nonoyama, Benzo(h)quinolin-10-yl-N iridium(III) complexes, *Bull. Chem. Soc. Jpn.* **1974**, *47*, 767–768.
- [21] S. Lamansky, P. Djurovich, D. Murphy, F. Abdel-Razzaq, R. Kwong, M. Venkatesh Perumal, B. Mmui, R. Bau, M. E. Thompson, Synthesis and characterization of phosphorescent cyclometalated iridium complexes, *Inorg. Chem.* **2001**, *40*, 1704–1711.
- [22] J. Jayabharathi, V. Thanikachalam, N. Srinivasan, K. Jayamoorthy, T. Venkatesh Perumal, An Intramolecular Charge Transfer Fluorescent Probe: Synthesis, Structure and Selective Fluorescent Sensing of Cu²⁺, *J. Fluoresc.* **2011**, *21*, 1813–1823.
- [23] S. Okada, K. Okinaka, H. Iwakaki, M. Furugori, M. Hashimoto, T. Mukaide, J. Kamatani, S. Igawa, A. Tsuboyama, T. Takiguchi, K. Ueno, Substituent effects of iridium complexes for highly efficient red OLEDs, *Dalton Trans.* **2005**, *9*, 1583–1590.
- [24] J. Jayabharathi, V. Thanikachalam, N. Srinivasan, M. Venkatesh Perumal, Physicochemical Studies Of Green Phosphorescent Light-Emitting Materials from Cyclometalated Heteroleptic Iridium (III) Complexes, *Spectrochim. Acta A* **2011**, *79*, 338–347.
- [25] K. Saravanan, N. Srinivasan, V. Thanikachalam, J. Jayabharathi, Synthesis and photophysics of some novel imidazole derivatives used as sensitive fluorescent chemisensors, *J. Fluoresc.* **2011**, *21*, 65–80.
- [26] J. Jayabharathi, V. Thanikachalam, K. Saravanan, Effect of substituents on the photoluminescence performance of Ir(III) complexes: Synthesis, electrochemistry and photophysical properties, *J. Photochem. Photobiol. A* **2009**, *208*, 13–20.
- [27] J. Jayabharathi, V. Thanikachalam, M. Venkatesh Perumal, N. Srinivasan, Fluorescence resonance energy transfer from a bioactive imidazole derivative 2-(1-phenyl-1H-imidazo[4,5-f][1,10]phenanthrolin-2-yl)phenol to a bioactive indoloquino lizine system, *Spectrochim. Acta A* **2011**, *9*, 236–244.
- [28] S. D. Cummings, R. Eisenberg, Tuning the Excited-State Properties of Platinum(II) Diimine, Dithiolate Complexes, *J. Am. Chem. Soc.* **1996**, *118*, 1949–1960.
- [29] R. R. Gagne, C. A. Koval, G. C. Lisensky, *Inorg. Chem.* **1980**, *19*, 2854.
- [30] P. J. Hay, *J. Phys. Chem. A* **2002**, *106*, 1634.
- [31] N. Li, P. Wang, S. L. Lai, W. Liu, C. S. Lee, S. T. Lee, Z. Liu, Synthesis of multiaryl-substituted pyridine derivatives and applications in non-doped deep-blue OLEDs as electron-transporting layer with high hole-blocking ability, *Adv. Mater.* **2010**, *27*, 527.
- [32] J. Pei, W.-L. Yu, J. Ni, Y.-H. Lai, W. Huang, A. J. Heeger, Thiophene-Based Conjugated Polymers for Light-Emitting Diodes: Effect of Aryl Groups on Photoluminescence Efficiency and Redox Behavior, *Macromolecules* **2001**, *34*, 7241–7248.
- [33] G. T. Hwang, H. S. Son, J. K. Ku, B. H. Kim, Synthesis and photophysical studies of bis-enediynes as tunable fluorophores, *J. Am. Chem. Soc.* **2003**, *125*, 11241–11248.
- [34] Z. Liu, M. Guan, Z. Bian, D. Nie, Z. Gong, Z. Li, C. Huang, Red Phosphorescent Iridium Complex Containing Carbazole-Functionalized β -Diketone for Highly Efficient Nondoped Organic Light Emitting Diodes, *Adv. Funct. Mater.* **2006**, *16*, 1441–1448.
- [35] J. Jayabharathi, V. Thanikachalam, N. Srinivasan, M. Venkatesh Perumal, Evidence for strong mixing between the LC and MLCT Excited states in some heteroleptic Iridium (III) Complexes, *J. Fluoresc.* **2011**, *21*, 1585–1597.